

**FULL PAPER**Applied  
Organometallic  
Chemistry**WILEY**

# Synthesis and characterization of $\text{Fe}_3\text{O}_4@\text{THAM-SO}_3\text{H}$ as a highly reusable nanocatalyst and its application for the synthesis of dihydropyrano[2,3-*c*]pyrazole derivatives

**Homayoun Faroughi Niya** | **Nourallah Hazeri** | **Malek Taher Maghsoodlou**

Department of Chemistry, Faculty of Science, University of Sistan and Baluchestan, P.O. Box 98135-674, Zahedan, Iran

**Correspondence**

Nourallah Hazeri, Department of Chemistry, Faculty of Science, University of Sistan and Baluchestan, P.O. Box 98135-674, Zahedan, Iran.  
Email: nhazeri@chem.usb.ac.ir; n\_hazeri@yahoo.com

**Funding information**

University of Sistan and Baluchestan

In this work, a new, green and beneficial nanomagnetic catalyst was easily fabricated using sulfuric acid as an acidic group on  $\text{Fe}_3\text{O}_4$  nanoparticles coated with tris (hydroxymethyl) aminomethane (THAM). The synthesized catalyst was characterized by FT-IR, TGA/DTG, XRD, TEM, EDS, VSM, and SEM analyses. Next, its catalytic activity was studied for the synthesis of dihydropyrano[2,3-*c*]pyrazole derivatives. This catalyst has advantages such as high catalytic activity, non-toxicity, easy separation from the reaction mixture using an external magnet and reuses for several times without significantly reducing in its catalytic activity.

**KEY WORDS**

$\text{Fe}_3\text{O}_4@\text{THAM-SO}_3\text{H}$ , heterogeneous nanocatalyst, magnetite nanoparticles, multicomponent reaction

## 1 | INTRODUCTION

In recent years, magnetic nanoparticles (MNPs) (especially superparamagnetic  $\text{Fe}_3\text{O}_4$  nanoparticles) are used in various applications in pharmaceutical industries and green chemistry such as drug delivery vehicles,<sup>[1,2]</sup> sensors,<sup>[3]</sup> and catalysts.<sup>[4,5]</sup> MNPs received considerable attention due to their superior characteristics such as high surface energies, high surface to volume ratios, easy recoverability, enhanced dispersion, high catalytic performance, and reusing without loss of their catalytic activity.<sup>[6–12]</sup> One of the most essential abilities of MNPs in organic chemistry is their catalyst role in multicomponent reactions (MCRs). The use of heterogeneous magnetic nanocatalyst has been widely reported. These nanocatalysts have small size and large external surface areas that allow great accessibility of substrates to the surface-bound active catalytic sites.<sup>[13–15]</sup> Also, their applications are increased due to their superior characteristics such as easily removable from the reaction mixture using an external magnet and reuse for several times

without significantly reducing in its catalytic activity.<sup>[16–20]</sup>

As a review of previous studies, many methods have been reported for sulfuric acid coupling as an acidic group on magnetic nanoparticles. Among them,  $\text{Fe}_3\text{O}_4@\text{APTES}@\text{isatin-SO}_3\text{H}$ ,<sup>[21]</sup>  $\text{CoFe}_2\text{O}_4@\text{SiO}_2-\text{SO}_3\text{H}$ ,<sup>[22]</sup>  $\text{Fe}_3\text{O}_4@\text{BNPs}@\text{SiO}_2-\text{SO}_3\text{H}$ ,<sup>[23]</sup>  $\text{Fe}_3\text{O}_4@\text{zeolite-SO}_3\text{H}$ ,<sup>[24]</sup>  $\text{Fe}_{3-x}\text{Ti}_x\text{O}_4-\text{SO}_3\text{H}$ <sup>[25]</sup> and  $\text{Fe}_3\text{O}_4@\text{GO-naphthalene-SO}_3\text{H}$ <sup>[26]</sup> are examples of catalysts.

Pyranopyrazoles and their derivatives such as dihydropyrano[2,3-*c*]pyrazole derivatives are an important class of heterocyclic compounds which have significant biological activities, such as anticancer,<sup>[27]</sup> vasodilatory<sup>[28]</sup> and bactericidal<sup>[29]</sup> activities. These molecules are also used as biodegradable agrochemicals and pharmaceutical ingredients.<sup>[30]</sup> Furthermore, dihydropyrano[2,3-*c*]pyrazole derivatives have attracted attention as molluscicidal agents<sup>[31,32]</sup> and potential insecticidal.<sup>[33]</sup>

In continue the development of synthesis of MNPs as a green catalyst for the production of pharmaceutical

compounds in one pot synthesis, we wish to propose a nanomagnetic catalyst using sulfuric acid as an acidic group on  $\text{Fe}_3\text{O}_4$  nanoparticles coated with THAM. Then, the synthesized nanocatalyst was used as a recyclable catalyst sorbents for one-pot synthesis of dihydropyrano[2,3-*c*]pyrazole derivatives from reaction between benzaldehyde (**1**), malononitrile (**2**) and 5-methyl-2-phenyl-2,4-dihydro-3*H*-pyrazol-3-one (**6**) or hydrazine hydrate (**3**) and acetoacetate (**4**) (Scheme 1).

## 2 | EXPERIMENTAL

### 2.1 | General

Melting points and FT-IR spectra of compounds were measured with an Electrothermal 9100 apparatus. The  $^1\text{H}$  NMR spectra were obtained on BRUKER DRX 300 and 400 MHz, using DMSO as a solvent. Ferrous chloride tetrahydrate ( $\text{FeCl}_2 \cdot 4\text{H}_2\text{O}$ ) and ferric chloride hexahydrate ( $\text{FeCl}_3 \cdot 6\text{H}_2\text{O}$ ) were obtained from Aldrich. Other reagents and solvents were obtained from Aldrich and Merck and were used without further purification.

### 2.2 | Synthesis of the magnetic $\text{Fe}_3\text{O}_4$ nanoparticles

$\text{Fe}_3\text{O}_4$  nanoparticles (NPs) have been synthesized by chemical coprecipitation method. Briefly,  $\text{FeCl}_2 \cdot 4\text{H}_2\text{O}$  (0.994 g, 5.0 mmol) and  $\text{FeCl}_3 \cdot 6\text{H}_2\text{O}$  (2.703 g, 10.0 mmol) were dissolved in 100 ml deionized water under nitrogen flow. Thereafter, 25% ammonia solution was added dropwise to the solution under vigorous stirring at 1000 rpm. After reaching the pH of 11, the mixture was stirred vigorously for 1 hr at room temperature. Finally, the nanoparticles obtained were separated and washed several times with ethanol and diethyl ether and dried for 2 hr at 60 °C in an oven.

### 2.3 | Synthesis of magnetite nanoparticles coated by tris (hydroxymethyl) aminomethane

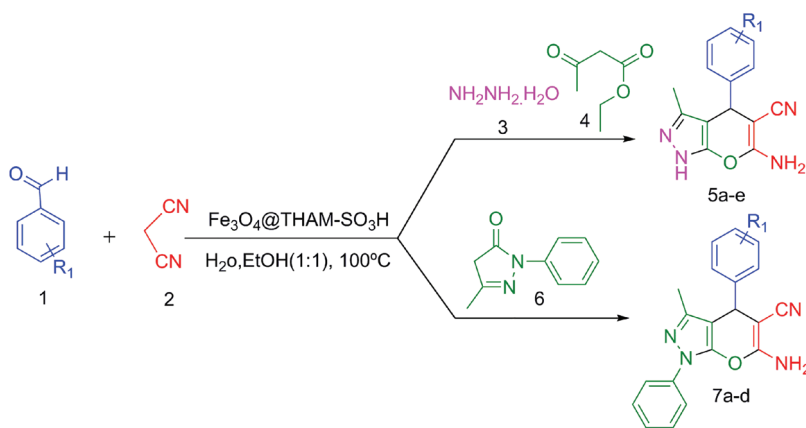
THAM-capped  $\text{Fe}_3\text{O}_4$  were prepared according to previous reports.<sup>[34]</sup> The synthesized  $\text{Fe}_3\text{O}_4$  (1.0 g) and 50 ml of ethanol were ultrasonically dispersed for 30 min. Then, to this suspension, 2.0 g of tris (hydroxymethyl) aminomethane (THAM) was added. The reaction mixture was stirred for 24 hr at 100 °C under  $\text{N}_2$  atmosphere. Finally, The resulting nanoparticles ( $\text{Fe}_3\text{O}_4@\text{THAM}$ ) were separated by an external magnet and washed several times with water to remove unreacted material and dried at 60 °C.

### 2.4 | Synthesis of $\text{Fe}_3\text{O}_4@\text{THAM-SO}_3\text{H}$

An amount of 1.0 g of the prepared magnetite  $\text{Fe}_3\text{O}_4@\text{THAM}$  nanoparticles was dispersed in 50 ml chloroform by ultrasonic bath for 20 min. Then, subsequently, chlorosulfonic acid (1.5 ml) was added dropwise and the resulting reaction mixture was stirred for 4 hr at room temperature under  $\text{N}_2$  atmosphere. The resulting nanoparticles ( $\text{Fe}_3\text{O}_4@\text{THAM-SO}_3\text{H}$ ) were separated by an external magnet and washed several times with ethanol to remove the remaining acid and dried at 60 °C.

### 2.5 | General procedure for four-component synthesis of dihydropyrano[2,3-*c*]pyrazole derivatives

Initially, the reactant ethyl acetoacetate (1.0 mmol) and hydrazine hydrate (1.0 mmol) were taken at room temperature until 3-methyl-2-pyrazoline-5-one was precipitated as white solid. Then, malononitrile (1.0 mmol), aromatic aldehyde (1.0 mmol) and  $\text{Fe}_3\text{O}_4@\text{THAM-SO}_3\text{H}$  (10 mg) in ethanol/water (1:1) was added to the reaction mixture at 100 °C and stirred for the appropriate time.



**S C H E M E 1**  $\text{Fe}_3\text{O}_4@\text{THAM-SO}_3\text{H}$  catalyzed the one-pot synthesis of dihydropyrano[2,3-*c*]pyrazoles derivatives

After the completion of the reaction which was monitored by TLC, the product was dissolved in hot ethanol and the catalyst separated by an external magnet, and the resulting solution was cooled to room temperature, the desired product precipitated and crystalized, then it was filtered.

## 2.6 | General procedure for three-component synthesis of dihydropyrano[2,3-c]pyrazole derivatives

A mixture of 5-methyl-2-phenyl-2,4-dihydro-3*H*-pyrazol-3-one (1.0 mmol), malononitrile (1.0 mmol), aldehydes (1.0 mmol) and Fe<sub>3</sub>O<sub>4</sub>@THAM-SO<sub>3</sub>H (10 mg) in ethanol/water (1:1) was stirred at 100 °C for the appropriate time. After the completion of the reaction which was monitored by TLC, the product was dissolved in hot ethanol and the catalyst separated by an external magnet, and the resulting solution was cooled to room temperature, the desired product precipitated and crystalized, then it was filtered. The spectra of selected compounds have been reported in supporting information.

## 2.7 | Selected spectra for seven known products are given below

### 2.7.1 | 6-Amino-1,4-dihydro-3-methyl-4-(2-chlorophenyl)pyrano[2,3-c]pyrazole-5-carbonitrile (5b)

FT-IR (KBr,  $\nu_{\text{max}}$ , cm<sup>-1</sup>): 3391 (NH<sub>2</sub>), 3357 (NH<sub>2</sub>), 3314 (NH), 2925(C-H<sub>aliphatic</sub>), 2190 (CN), 1654 (C=N), 1272 (C-O). <sup>1</sup>H NMR (300 MHz, DMSO) δ = 1.82 (s, 3H, CH<sub>3</sub>), 5.12 (s, 1H, C-H), 7.00 (s, 2H, NH<sub>2</sub>), 7.22–7.66 (m, 4H, Ar-H), 12.18 (s, 1H, NH).

### 2.7.2 | 6-Amino-1,4-dihydro-3-methyl-4-(2-nitrophenyl)pyrano[2,3-c]pyrazole-5-carbonitrile (5c)

FT-IR (KBr,  $\nu_{\text{max}}$ , cm<sup>-1</sup>): 3414 (NH<sub>2</sub>), 3376 (NH<sub>2</sub>), 3315 (NH), 2186 (CN), 1158 (C-O). <sup>1</sup>H NMR (300 MHz, DMSO) δ = 1.79 (s, 3H, CH<sub>3</sub>), 5.11 (s, 1H, CH), 7.05 (s, 2H, NH<sub>2</sub>), 7.33–7.92 (m, 4H, Ar-H), 12.22 (s, 1H, NH).

### 2.7.3 | 6-amino-1,4-dihydro-3-methyl-4-(3,4-dimethoxyphenyl)pyrano[2,3-c]pyrazole-5-carbonitrile (5d)

FT-IR (KBr,  $\nu_{\text{max}}$ , cm<sup>-1</sup>): 3456 (NH<sub>2</sub>), 3346 (NH<sub>2</sub>), 3229 (NH), 2971(C-H<sub>aliphatic</sub>), 2209 (CN), 1568, 1642 (C=C),

752, 853 (C-H). <sup>1</sup>H-NMR (300 MHz, DMSO) δ = 1.83 (s, 3H, CH<sub>3</sub>), 3.66 (s, 3H, OCH<sub>3</sub>), 3.79 (s, 3H, OCH<sub>3</sub>), 4.94 (s, 1H, CH), 6.54 (d, J = 3 Hz, 1H, Ar-H), 6.79 (dd, J<sub>1</sub> = 8.7 Hz, J<sub>2</sub> = 3 Hz, 1H, Ar-H), 6.84 (s, 2H, NH<sub>2</sub>), 6.95 (d, J = 9 Hz, 1H, Ar-H), 12.03 (s, 1H, N-H).

### 2.7.4 | 6-amino-1,4-dihydro-3-methyl-4-(4-bromophenyl)pyrano[2,3-c]pyrazole-5-carbonitrile (5e)

<sup>1</sup>H-NMR (300 MHz, DMSO) δ = 1.80 (s, 3H, CH<sub>3</sub>), 4.63 (s, 1H, CH), 6.96 (s, 2H, NH<sub>2</sub>), 7.15 (d, J = 8 Hz, 2H, Ar-H), 7.54 (d, J = 8 Hz, 2H, Ar-H), 12.17 (s, 1H, N-H).

### 2.7.5 | 6-Amino-3-methyl-1,4-diphenyl-1,4-dihdropyrano[2,3-c]pyrazole-5-carbonitrile (7a)

FT-IR (KBr,  $\nu_{\text{max}}$ , cm<sup>-1</sup>): 3471 (NH<sub>2</sub>), 3324 (NH), 3063 (C-H<sub>aromatic</sub>), 2919 (C-H<sub>aliphatic</sub>), 2198 (CN), 1592, 1516 (C=C), 685, 753 (C-H). <sup>1</sup>H-NMR (300 MHz, DMSO): (δ, ppm): 1.80 (s, 3H, CH<sub>3</sub>), 4.70 (s, 1H, CH), 7.23 (s, 2H, NH<sub>2</sub>), 7.26–7.40 (m, 6H, Ar-H), 7.51 (t, J = 8 Hz, 2H, Ar-H), 7.81 (d, J = 9 Hz, 2H, Ar-H).

### 2.7.6 | 6-Amino-1,4-dihydro-3-methyl-4-(2,4-dichlorophenyl)-1-phenylpyrano[2,3-c]pyrazole-5-carbonitrile (7b)

<sup>1</sup>H NMR (400 MHz, DMSO): δ = 1.81 (s, 3H, CH<sub>3</sub>), 4.74 (s, 1H, CH), 7.31–7.44 (m, 5H, NH<sub>2</sub> and ArH), 7.48–7.52 (m, 2H, ArH), 7.62 (s, 1H, ArH), 7.78 (d, J = 8 Hz, 2H, ArH).

### 2.7.7 | 6-amino-1,4-dihydro-3-methyl-4-(4-chlorophenyl)-1-phenylpyrano[2,3-c]pyrazole-5-carbonitrile (7c)

<sup>1</sup>H NMR (400 MHz, DMSO): δ = 1.79 (s, 3H, CH<sub>3</sub>), 5.16 (s, 1H, CH), 7.28–7.79 (m, 9H, ArH), 7.81 (s, 2H, NH<sub>2</sub>).

## 3 | RESULTS AND DISCUSSION

### 3.1 | Synthesis and characterization of catalyst

In this work, we prepared a new nanocatalyst (Fe<sub>3</sub>O<sub>4</sub>@THAM-SO<sub>3</sub>H) by following the method shown

in Scheme 2. In the first step, The  $\text{Fe}_3\text{O}_4$  MNPs were prepared by chemical coprecipitation method. Then, chlorosulfonic acid was coated on the surface of magnetite nanoparticles using tris (hydroxymethyl) aminomethane. The synthesized nanocatalyst was characterized using several techniques, including Fourier transform infrared (FT-IR), X-ray diffraction (XRD), thermogravimetric (TGA), differential thermal analysis (DTA), vibrating sample magnetometer (VSM), field emission scanning electron microscopy (FE-SEM), X-ray spectroscopy (EDS), and TEM analyses.

The determination of the size and morphology of the  $\text{Fe}_3\text{O}_4@\text{THAM-SO}_3\text{H}$  was performed by FESEM. As shown in Figure 1, The particles of uncoated  $\text{Fe}_3\text{O}_4$  and  $\text{Fe}_3\text{O}_4@\text{THAM-SO}_3\text{H}$  are uniform in both shape and size. The FESEM image of the nanocatalyst ( $\text{Fe}_3\text{O}_4@\text{THAM-SO}_3\text{H}$ ) showed the spherical-shaped nanoparticles and an average size of approximately 14 nm. The size histogram of  $\text{Fe}_3\text{O}_4$  (a) and  $\text{Fe}_3\text{O}_4@\text{THAM-SO}_3\text{H}$  (b) was constructed by measuring 200 particles that appear in the FESEM image (Figure 2).

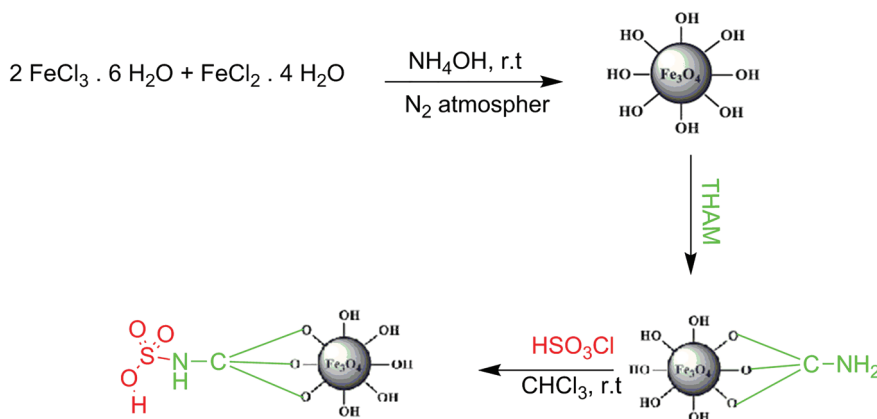
The EDS spectrum of  $\text{Fe}_3\text{O}_4@\text{THAM-SO}_3\text{H}$  exhibited in Figure 3. This spectrum showed the presence of oxygen (O, 25%), sulfur (S, 2.2%), nitrogen (N, 1.2%), carbon (C, 17.3%) and iron (Fe, 54.3%) elements. This spectrum is proof for the fact that the organic layer ( $\text{THAM-SO}_3\text{H}$ ) was immobilized onto the  $\text{Fe}_3\text{O}_4$  nanoparticles.

TEM images, which is presented in Figure 4, clearly demonstrates that the nanocatalyst was composed of two parts, brighter and darker parts (core-shell structure). The brighter parts of the image are likely related to the organic layer anchored to the surface of the  $\text{Fe}_3\text{O}_4$  NPs and the darker parts correspond to magnetic nanoparticles. Also, the TEM image of  $\text{Fe}_3\text{O}_4@\text{THAM-SO}_3\text{H}$  exhibits that the morphology of nanoparticles is almost spherical with a narrow size distribution of about 11 nm (Figure 5), which confirmed the achieved SEM data.

The characterization of  $\text{Fe}_3\text{O}_4@\text{THAM-SO}_3\text{H}$  was confirmed by FT-IR spectrum (Figure 6) which showed spectra of  $\text{Fe}_3\text{O}_4$  (a) and  $\text{Fe}_3\text{O}_4@\text{THAM-SO}_3\text{H}$  (b). In Figure 6a can be seen the Fe-O stretching vibration of  $\text{Fe}_3\text{O}_4$  at  $550\text{--}650\text{ cm}^{-1}$ . Also, two peaks at  $1618\text{ cm}^{-1}$  and  $3374\text{ cm}^{-1}$  are attributed to bending vibration and stretching vibration of the OH functional groups on the surface of  $\text{Fe}_3\text{O}_4$ , respectively. The spectrum of  $\text{Fe}_3\text{O}_4@\text{THAM-SO}_3\text{H}$  (Figure 6b) shows some bands in  $1000\text{--}1250\text{ cm}^{-1}$  which are attributed to the absorption S-O and S=O stretching bands of  $-\text{SO}_3\text{H}$  moiety on  $\text{Fe}_3\text{O}_4@\text{THAM-SO}_3\text{H}$  surface. In addition, the peak at  $3405\text{ cm}^{-1}$  in the spectrum of  $\text{Fe}_3\text{O}_4@\text{THAM-SO}_3\text{H}$  was probably attributed to the  $-\text{SO}_2\text{-OH}$  groups, which is overlapped by the Fe-OH stretching vibration.<sup>[21]</sup>

The thermal stability of  $\text{Fe}_3\text{O}_4@\text{THAM-SO}_3\text{H}$  nanoparticles was studied by TG/DTG analysis in the decomposition area of  $0\text{--}600\text{ }^\circ\text{C}$  with a heating rate of  $10\text{ }^\circ\text{C}$  per minute under nitrogen atmosphere (Figure 7). As can be seen,  $\text{Fe}_3\text{O}_4@\text{THAM-SO}_3\text{H}$  nanoparticles displayed four weight-loss steps. The initial weight loss (4.82%) from room temperature to  $180\text{ }^\circ\text{C}$  is related to loss of physically adsorbed solvent and the surface hydroxyl groups. The second weight loss (5.09%) between  $180$  and  $330\text{ }^\circ\text{C}$  is due to thermal decomposition of acidic functional groups ( $\text{SO}_3\text{H}$ ) of the nanocatalyst. The other organic moiety grafted on the  $\text{Fe}_3\text{O}_4$  NPs decomposed at elevated temperatures (weight loss 11.41%). The total weight loss was computed to be 16.5%. In accordance with this mass loss, it was computed that the amount of 0.85 mmol of the organic layer ( $\text{THAM-SO}_3\text{H}$ ) was loaded on 1 g of  $\text{Fe}_3\text{O}_4$  nanoparticles. Furthermore, the DTG curve shows that the decomposition of the organic structure mainly happened at  $250\text{ }^\circ\text{C}$ . So, the  $\text{Fe}_3\text{O}_4@\text{THAM-SO}_3\text{H}$  is stable below this temperature.

The XRD pattern of  $\text{Fe}_3\text{O}_4@\text{THAM-SO}_3\text{H}$  and  $\text{Fe}_3\text{O}_4$  was investigated in the domain of 5–80 degrees (Figure 8). The powder XRD pattern of the  $\text{Fe}_3\text{O}_4$



**S C H E M E 2** Preparation of  $\text{Fe}_3\text{O}_4@\text{THAM-SO}_3\text{H}$

**FIGURE 1** SEM images of Fe<sub>3</sub>O<sub>4</sub> (a) and Fe<sub>3</sub>O<sub>4</sub>@THAM-SO<sub>3</sub>H (b)

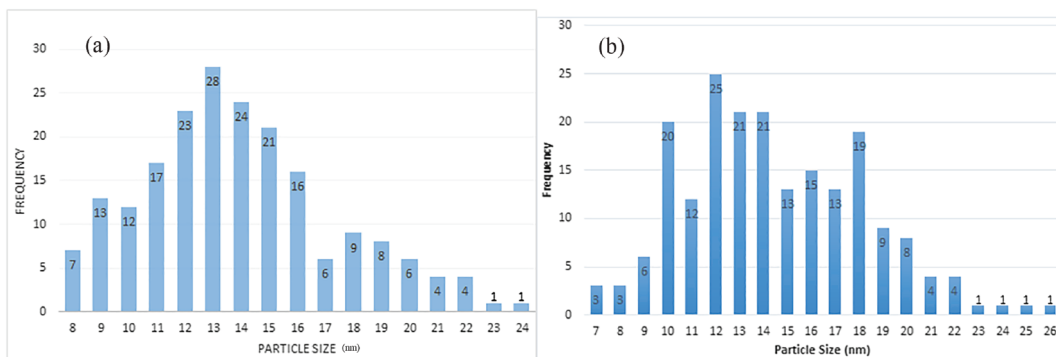
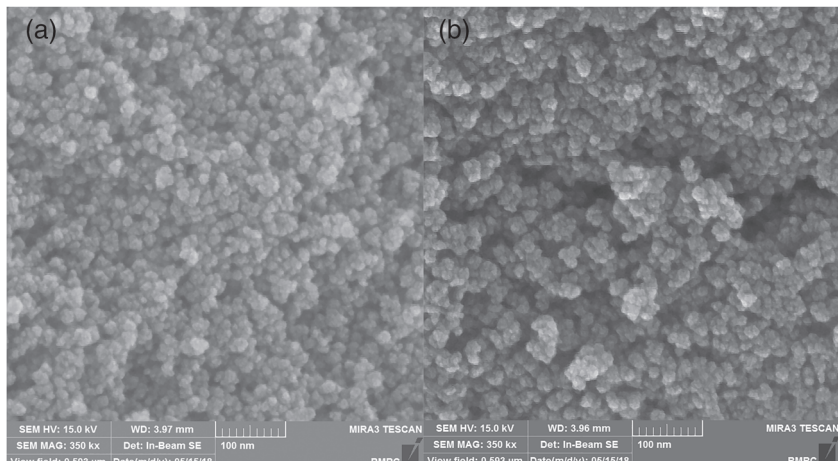


**FIGURE 2** The size histogram of Fe<sub>3</sub>O<sub>4</sub> (a) and Fe<sub>3</sub>O<sub>4</sub>@THAM-SO<sub>3</sub> (b)

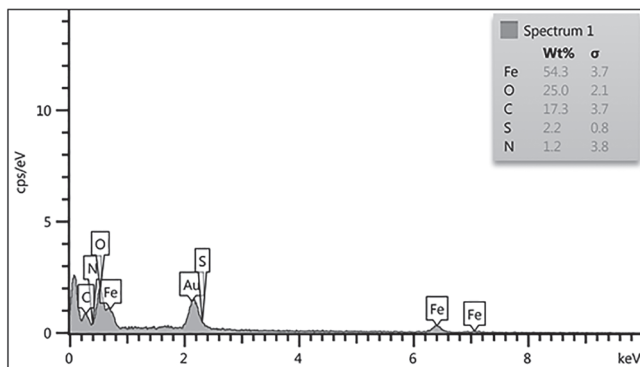


**FIGURE 3** EDS spectrum of Fe<sub>3</sub>O<sub>4</sub>@THAM-SO<sub>3</sub>H

(Figure 8a) exhibited diffraction peaks at  $2\theta = 30.03^\circ$ ,  $35.68^\circ$ ,  $43.36^\circ$ ,  $53.85^\circ$ ,  $57.35^\circ$ ,  $62.79^\circ$  and  $74.43^\circ$ , which are associated with corresponding indices of (2 0 2), (3 1 1), (4 0 0), (4 2 2), (5 1 1), (4 4 0) and (6 6 0), respectively. In the XRD pattern of Fe<sub>3</sub>O<sub>4</sub>@THAM-SO<sub>3</sub>H (Figure 8b), an additional broad peak at region lower than  $20^\circ$  is seen which can be attributed to the existence of amorphous organic layer (THAM-SO<sub>3</sub>H) that was immobilized onto the Fe<sub>3</sub>O<sub>4</sub> nanoparticles.

The magnetic properties of Fe<sub>3</sub>O<sub>4</sub> NPs and Fe<sub>3</sub>O<sub>4</sub>@THAM-SO<sub>3</sub>H were analyzed via VSM at room temperature (Figure 9). The M(H) hysteresis loop was completely reversible. Hence, these results indicate that nanocatalyst possesses sufficient superparamagnetism. The magnetic saturation (Ms) values of Fe<sub>3</sub>O<sub>4</sub> NPs and Fe<sub>3</sub>O<sub>4</sub>@THAM-SO<sub>3</sub>H are 116.6 and 42.3 emu g<sup>-1</sup>, respectively. The decrease of MS for the synthesized nanocatalyst (Fe<sub>3</sub>O<sub>4</sub>@THAM-SO<sub>3</sub>H) is due to the non-magnetic nature of the organic layer anchored to the surface of the Fe<sub>3</sub>O<sub>4</sub> NPs.

### 3.2 | Catalytic application of Fe<sub>3</sub>O<sub>4</sub>@THAM-SO<sub>3</sub>H

In order to evaluate the catalytic activity of the Fe<sub>3</sub>O<sub>4</sub>@THAM-SO<sub>3</sub>H nanoparticles, they were used in the synthesis of dihydropyrano[2,3-c]pyrazole derivatives (Scheme 1). To find the optimal reaction conditions, the four-component reaction of benzaldehyde (**1**), malononitrile (**2**), hydrazine hydrate (**3**) and acetoacetate (**4**) was chosen as a model reaction. Initially, the influence of a variety of solvents was investigated using

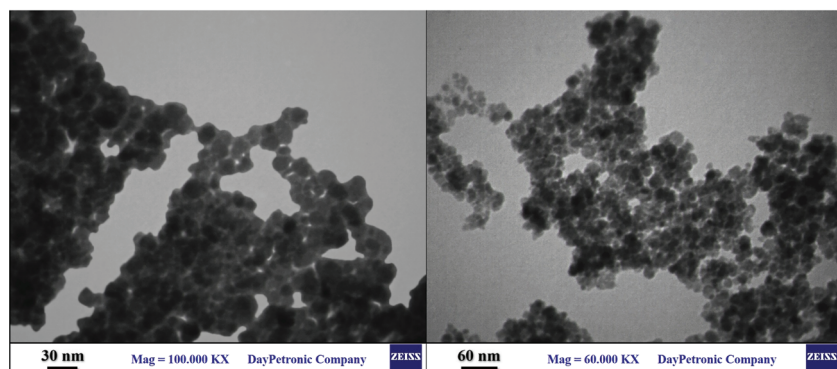


**FIGURE 4** TEM images of Fe<sub>3</sub>O<sub>4</sub>@THAM-SO<sub>3</sub>H

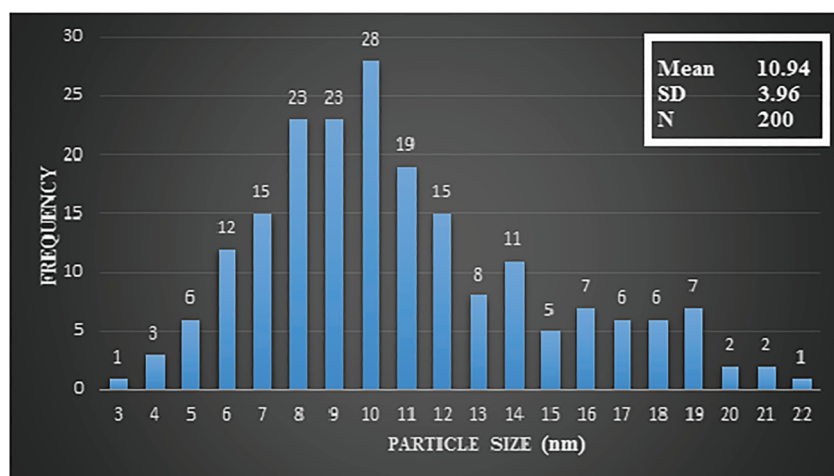


**FIGURE 5** The size histogram of Fe<sub>3</sub>O<sub>4</sub>@THAM-SO<sub>3</sub>H

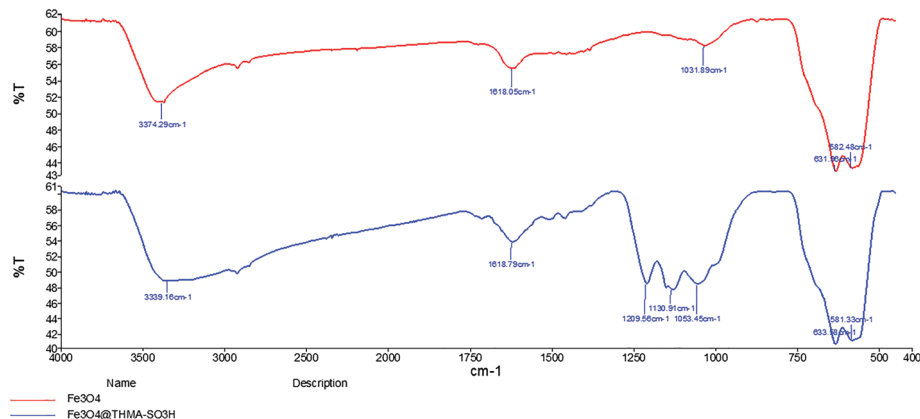


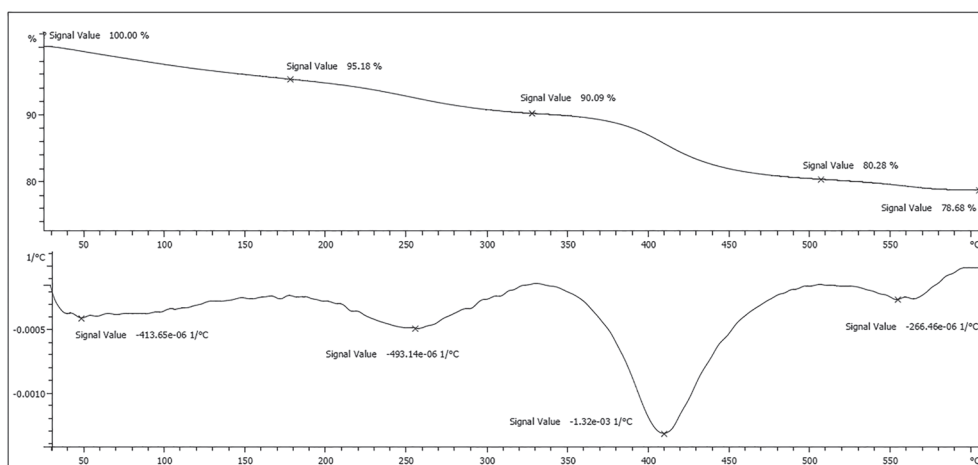
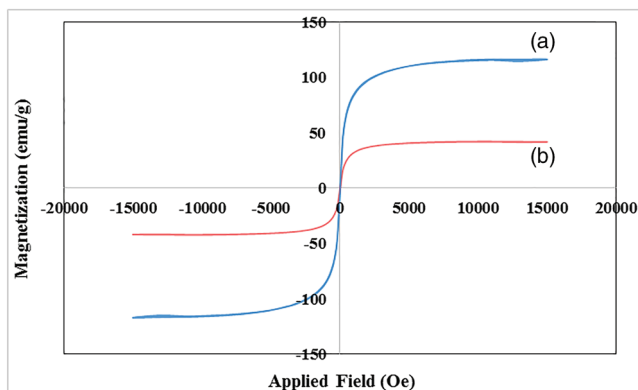
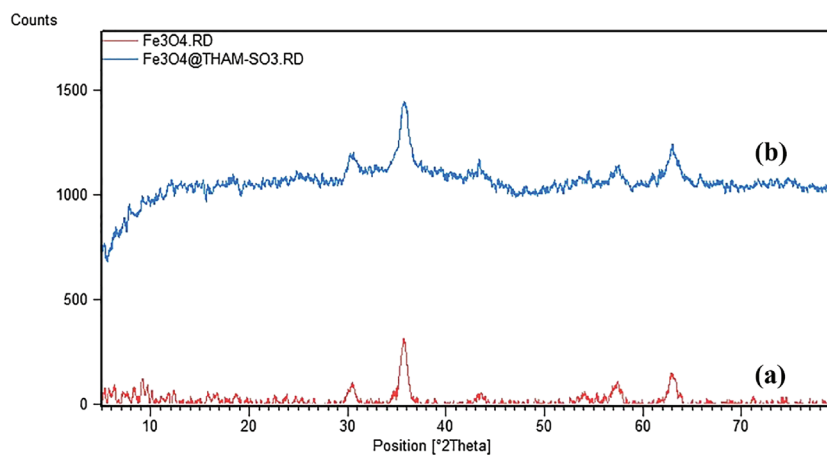
**FIGURE 6** FT-IR spectra of Fe<sub>3</sub>O<sub>4</sub> (a) and Fe<sub>3</sub>O<sub>4</sub>@THAM-SO<sub>3</sub>H (b)

various solvents such as ethanol, water, or mixture of ethanol:water (1:1). All of the results are registered in Table 1. Among the studied solvents, mixture of ethanol:water (1:1) exhibited the most potent effect on the model reaction (Table 1, entry 2).

In the next step, the model reaction was performed with various amounts of nanoparticles (5, 7.5, 10, 15 mg). All of the results are registered in Table 2. The best result was obtained in the presence of 10 mg of Fe<sub>3</sub>O<sub>4</sub>@THAM-SO<sub>3</sub>H as a catalyst which confirmed the catalytic activity of Fe<sub>3</sub>O<sub>4</sub>@THAM-SO<sub>3</sub>H nanoparticles. Finally, the effect

of temperature was studied. Based on our experimental results, the best result is obtained in ethanol:water (1:1) at 100 °C in the presence of 10 mg of Fe<sub>3</sub>O<sub>4</sub>@THAM-SO<sub>3</sub>H for 10 min. In these conditions, the desired product was obtained at 80% yields (Table 2, entry 9).

After optimizing the reaction conditions, of benzaldehyde (**1**), malononitrile (**2**), hydrazine hydrate (**3**) and acetoacetate (**4**) under optimized conditions for preparation of dihydropyrano[2,3-*c*]pyrazole derivatives was investigated. Interestingly, a variety of aromatic aldehydes including, *para*, *meta*, *ortho*-substituted were used

**FIGURE 7** TGA and DTG curves of Fe<sub>3</sub>O<sub>4</sub>@THAM-SO<sub>3</sub>H**FIGURE 8** XRD pattern of Fe<sub>3</sub>O<sub>4</sub> (a) and Fe<sub>3</sub>O<sub>4</sub>@THAM-SO<sub>3</sub>H (b)**FIGURE 9** VSM spectra of Fe<sub>3</sub>O<sub>4</sub> (a) and Fe<sub>3</sub>O<sub>4</sub>@THAM-SO<sub>3</sub>H (b)**TABLE 1** Optimization of solvent at 60 °C

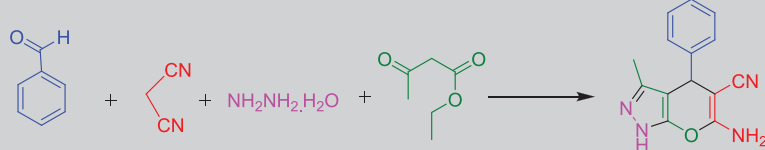
Entry	Solvent	Time (min)	Yield (%)
1	EtOH	50	37
2	H <sub>2</sub> O:EtOH (1:1)	30	67
3	H <sub>2</sub> O	35	66

and corresponding products were synthesized in excellent yields at short reaction times (Table 3).

A proposed mechanism for the synthesis of dihydropyrano[2,3-*c*]pyrazoles is provided in Scheme 3. In the first step, the electrophilicity of the carbonyl group of aldehyde (**1**) was increased by the proton from Fe<sub>3</sub>O<sub>4</sub>@THAM-SO<sub>3</sub>H. Next, the Knoevenagel condensation of malononitrile (**2**) with activated aldehyde generates 2-benzylidenemalononitrile intermediate (**a**). In the second step, Michael addition of 5-methyl-2-phenyl-2,4-dihydro-3*H*-pyrazol-3-one (**6**) or pyrazolone (**b**) (from the reaction between ethyl acetoacetate (**4**) and hydrazine hydrate (**3**)) to 2-benzylidene malononitrile intermediate (**a**), followed by continuous intramolecular cyclization happen to give the intermediate (**d**). Finally, tautomerization affords the corresponding product.

### 3.3 | Catalyst recovery and reuse

The recyclability and stability of the catalyst was checked using the three-component reaction of

**TABLE 2** Effect of the catalyst amount and temperature on the model reaction

Entry	Catalyst (gr)	Temperature (°C)	Time (min)	Yield (%)
1	No catalyst	60	40	56
2	0.005	60	40	50
3	0.0075	60	40	53
4	0.01	60	30	67
5	0.015	60	30	55
7	0.01	70	30	70
8	0.01	90	20	68
<b>9</b>	<b>0.01</b>	<b>100</b>	<b>10</b>	<b>80</b>
10	0.01	110	10	75

4-chlorobenzaldehyde, malononitrile, and 5-methyl-2-phenyl-2,4-dihydro-3*H*-pyrazol-3-one, using the recycled catalyst under the optimized conditions. After completion of the reaction, the product was dissolved in hot ethanol (30 ml) and the catalyst separated by an external magnet and washed with ethanol for three

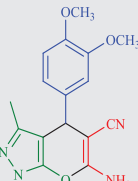
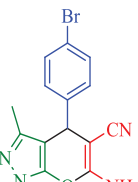
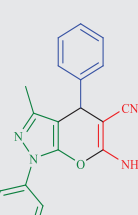
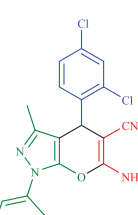
times to remove any organic moieties present and dried at 60 °C. The catalyst was used directly in the next run. As shown in Figure 10, the catalyst could be reused eight times with no significant reduction in its activities. This small decrease can be attributed to the loss of catalyst after every recycling.

**TABLE 3** Synthesis of dihydropyrano[2,3-*c*]pyrazole derivatives in the presence of Fe<sub>3</sub>O<sub>4</sub>@THAM-SO<sub>3</sub>H (0.01 g) in water/ethanol (1:1) at 100 °C

Entry	Product	Time (min)	Yield (%)	M.p (°C)	M.p (°C) [Lit.] Ref.
1		10	80	244–246	243–245 <sup>[35]</sup>
	<b>5a</b>				
2		15	75	143–145	145–147 <sup>[35]</sup>
	<b>5b</b>				
3		25	69	226–228	227–228 <sup>[36]</sup>

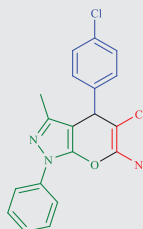
(Continues)

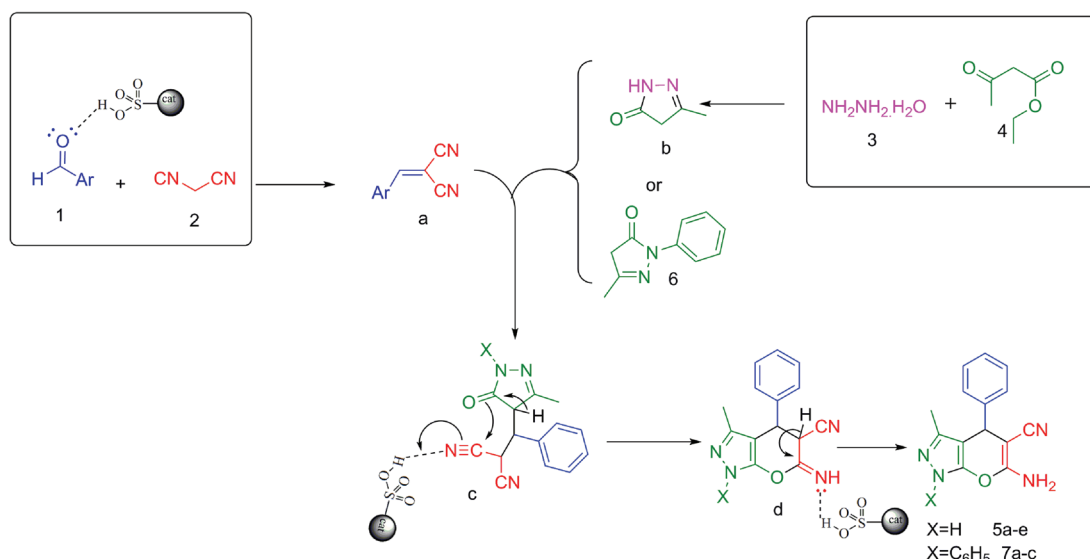
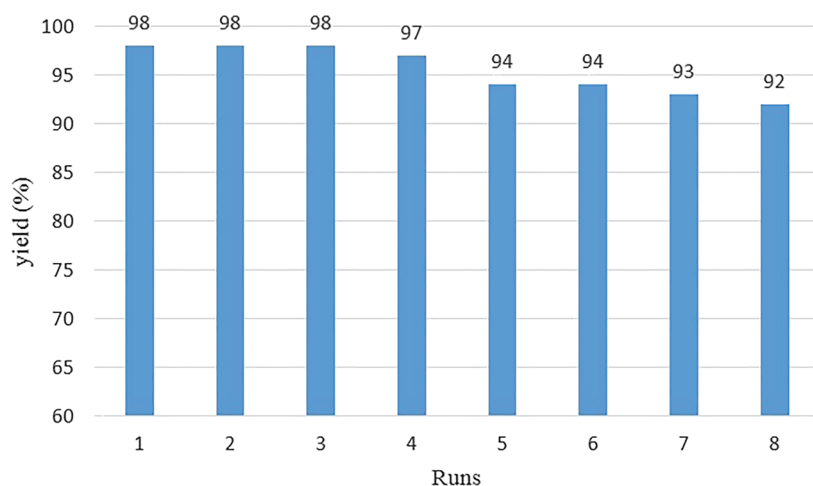
**TABLE 3** (Continued)

Entry	Product	Time (min)	Yield (%)	M.p (°C)	M.p (°C) [Lit.] Ref.
					
4	<b>5c</b> <b>5c</b>	10	81	190–193	189–193 <sup>[35]</sup>
					
	<b>5d</b> <b>5d</b>	5	85	180–181	178–180 <sup>[35]</sup>
5					
	<b>5e</b> <b>5e</b>	20	82	165–168	167–169 <sup>[35]</sup>
6					
	<b>7a</b>	10	88	182–184	181–183 <sup>[35]</sup>
7					
	<b>7b</b> <b>7b</b>				

(Continues)

**TABLE 3** (Continued)

Entry	Product	Time (min)	Yield (%)	M.p (°C)	M.p (°C) [Lit.] Ref.
8	 <b>7c</b>	5	98	169–171	170–172 <sup>[35]</sup>

**SCHM**E 3 Proposed mechanism for the synthesis of dihydropyrano[2,3-c]pyrazoles**FIGURE 10** Reusability of the nanocatalyst in the synthesis of 6-amino-1,4-dihydro-3-methyl-4-(4-chlorophenyl)-1-phenylpyrano[2,3-c]pyrazole-5-carbonitrile

## 4 | CONCLUSIONS

In this study, The Fe<sub>3</sub>O<sub>4</sub> nanoparticles (NPs) was synthesized easily by chemical coprecipitation method at room temperature. The synthesis of Fe<sub>3</sub>O<sub>4</sub> NPs at room temperature has some advantage such as better magnetic properties and avoids Fe<sub>3</sub>O<sub>4</sub> to γ-Fe<sub>2</sub>O<sub>3</sub> conversion. Then, Fe<sub>3</sub>O<sub>4</sub>@THAM-SO<sub>3</sub>H as a magnetically retrievable nanocatalyst was synthesized and characterized by several analyses including FT-IR, XRD, SEM, EDS, TEM, VSM, and TG/DTG. The synthesized nanocatalyst was successfully employed in the synthesis of dihydropyrano[2,3-c]pyrazole derivatives. This heterogeneous nanocatalyst has the following advantages: easy product separation and purification, reusability for eight reactions cycles without any significant decrease in catalytic activity, eco-friendly nature that make it sustainable, attractive and economic in agreement with some green chemistry protocols.

## ACKNOWLEDGEMENTS

The authors gratefully appreciate the financial support from the Research Council of University of Sistan and Baluchestan.

## ORCID

Nourallah Hazeri  <https://orcid.org/0000-0002-0560-7245>

Malek Taher Maghsoodlou  <https://orcid.org/0000-0002-4454-8049>

## REFERENCES

- [1] S. Laurent, D. Forge, M. Port, A. Roch, C. Robic, L. V. Elst, R. N. Muller, *Chem. Rev.* **2008**, *108*, 2064.
- [2] A. K. Gupta, M. Gupta, *Biomaterials* **2005**, *26*, 3995.
- [3] O. J. Cayre, N. Chagneux, S. Biggs, *Soft Matter* **2011**, *7*, 2211.
- [4] F. Tajifirooz, A. Davoodnia, M. Pordel, M. Ebrahimi, A. Khojastehnezhad, *Appl. Organomet. Chem.* **2017**, *32*, e3930.
- [5] S. Phadtare, A. Kumar, V. P. Vinod, C. Dash, D. V. Palaskar, M. Rao, P. G. Shukla, S. Sivaram, M. Sastry, *Chem. Mater.* **2003**, *15*, 1944.
- [6] S. Shylesh, V. Schnemann, W. R. Thiel, *Angew. Chem. Int. Ed.* **2010**, *49*, 3428.
- [7] D. Wang, D. Astruc, *Chem. Rev.* **2014**, *114*, 6949.
- [8] M. Mokhtary, J. Iran, *Chem. Soc.* **2016**, *13*, 1827.
- [9] T. Cheng, D. Zhang, H. Li, G. Liu, *Green Chem.* **2014**, *16*, 3401.
- [10] B. Karimi, F. Mansouri, H. M. Mirzaei, *ChemCatChem* **2015**, *7*, 1736.
- [11] C. W. Lim, I. S. Lee, *Nano Today* **2010**, *5*, 412.
- [12] (a) S. Payra, A. Saha, S. Banerjee, *J. Nanosci. Nanotechnol.* **2017**, *17*, 4432. (b) A. Maleki, *Tetrahedron* **2012**, *68*, 7827. (c) A. Maleki, T. Kari, M. Aghaei, *J. Porous Mater.* **2017**, *24*, 1481. (d) A. Maleki, *RSC Adv.* **2014**, *4*, 64169.
- [13] B. Rác, A. Molnar, P. Forgo, M. Mohai, I. Bertóti, *J. Mol. Catal. A: Chem.* **2006**, *244*, 46.

- [14] V. Moodley, S. Maddila, S. B. Jonnalagadda, W. E. van Zyl, *New J. Chem.* **2017**, *41*, 6455.
- [15] S. Safaei, I. Mohammadpoor-Baltork, A. R. Khosropour, M. Moghadam, S. Tangestaninejad, V. Mirkhani, *Catal. Sci. Technol.* **2013**, *3*, 2717.
- [16] H. R. Shaterian, M. Mohammadnia, *Res. Chem. Intermed.* **2013**, *39*, 4221.
- [17] A. R. Moosavi-Zare, M. A. Zolfigol, M. Zarei, A. Zare, V. Khakyzadeh, *J. Mol. Liq.* **2015**, *211*, 373.
- [18] H. R. Shaterian, F. Mordini, *Res. Chem. Intermed.* **2015**, *41*, 291.
- [19] F. Khorami, H. R. Shaterian, *Res. Chem. Intermed.* **2015**, *41*, 3171.
- [20] H. R. Shaterian, A. Hosseiniyan, *Res. Chem. Intermed.* **2014**, *40*, 3011.
- [21] S. Sajjadifar, Z. Gheisarzadeh, *Appl. Organomet. Chem.* **2019**, *33*, e4602.
- [22] S. Mandal, S. Hazra, S. Sarkar, C. Bodhak, A. Pramanik, *Appl. Organomet. Chem.* **2019**, *33*, e4702.
- [23] M. G. Kermanshahi, K. Bahrami, *RSC Adv.* **2019**, *9*, 36103.
- [24] M. Kalhor, Z. Zarnegar, F. Janghorban, S. A. Mirshokraei, *Res. Chem. Intermed.* **2019**, *1*.
- [25] D. Azarifar, Y. Abbasi, M. Jaymand, M. A. Zolfigol, M. Ghaemi, O. Badalkhani, *J. Organomet. Chem.* **2019**.
- [26] M. Khaleghi-Abbasabadi, D. Azarifar, *Res. Chem. Intermed.* **2019**, *45*, 2095.
- [27] M. R. Nadia, Y. K. Nahed, A. A. Fahmyb, A. A. F. El-Sayed, *Pharma Chem.* **2010**, *2*, 400.
- [28] V. K. Ahluwalia, A. Dahiya, V. Garg, *Indian J. Chem.* **1997**, *36B*, 88.
- [29] M. N. Nasr, M. M. Gineinah, *Arch. Pharm. Med. Chem.* **2002**, *335*, 289.
- [30] H. Junek, H. Aigner, *Chem. Ber.* **1973**, *106*, 914.
- [31] F. M. Abdelrazeck, P. Metz, N. H. Metwally, S. F. El-Mahrouky, *Arch. Pharm.* **2006**, *339*, 456.
- [32] A. Siddekh, A. Nizam, M. A. Pasha, *Spectrochim. Acta B* **2011**, *81*, 431.
- [33] E. S. El-Tamany, F. A. El-Shahed, B. H. Mohamed, *J. Serb. Chem. Soc.* **1999**, *64*, 9.
- [34] S. M. El-Sigeny, M. F. Abou Taleb, *Life Sci. J.* **2015**, *12*, 161.
- [35] H. Pejman, N. Hazeri, M. Fatahpour, H. Faroughi Niya, *Rev. Roum. Chim.* **2019**, *64*, 241.
- [36] A. Maleki, V. Eskandarpour, *J. Iran Chem. Soc.* **2019**, *16*, 1459.

## SUPPORTING INFORMATION

Additional supporting information may be found online in the Supporting Information section at the end of this article.

**How to cite this article:** Faroughi Niya H, Hazeri N, Maghsoodlou MT. Synthesis and characterization of Fe<sub>3</sub>O<sub>4</sub>@THAM-SO<sub>3</sub>H as a highly reusable nanocatalyst and its application for the synthesis of dihydropyrano[2,3-c]pyrazole derivatives. *Appl. Organometal. Chem.* 2020;e5472. <https://doi.org/10.1002/aoc.5472>